El-Houjeiri and Biondini et.al 2020 Supplementary Figures and Tables legends

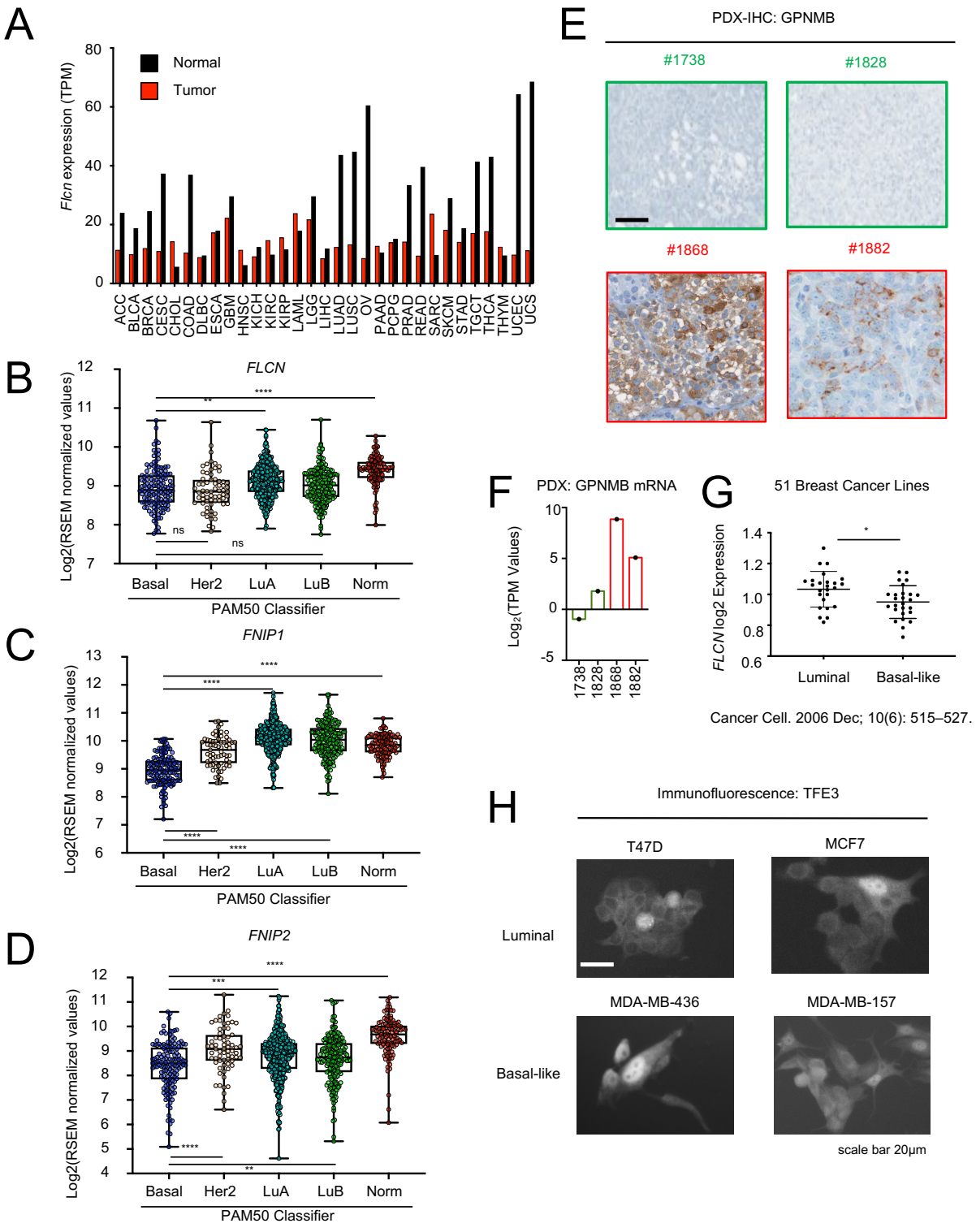

Supplemental Figure 1 (related to Figure 1). FLCN, FNIP1 and FNIP2 are downregulated in basal-like breast cancer models compared to luminal subtypes. (A) FLCN gene expression profile across different tumor samples and paired normal tissues from TCGA dataset (http://gepia2.cancer-pku.cn/#general). The height of each bar represents the median expression in the specified tumor types or normal tissue. ACC: Adrenocortical carcinoma; BLCA: Bladder Urothelial Carcinoma; BRCA: Breast invasive carcinoma; CESC: Cervical squamous cell carcinoma and endocervical adenocarcinoma; CHOL: Cholangiocarcinoma; LCML: Chronic Myelogenous Leukemia; COAD: Colon adenocarcinoma; CNTL: Controls; ESCA: Esophageal carcinoma; FPPP: FFPE Pilot Phase II; GBM: Glioblastoma multiform, HNSC: Head and Neck squamous cell carcinoma; KICH: Kidney Chromophobe; KIRC: Kidney renal clear cell carcinoma; KIRP: Kidney renal papillary cell carcinoma; LGG: Brain Lower; Grade Glioma; LIHC: Liver hepatocellular carcinoma; LUAD: Lung adenocarcinoma; LUSC: Lung squamous cell carcinoma; DLBC: Lymphoid Neoplasm Diffuse Large B-cell Lymphoma; MESO: Mesothelioma; MISC: Miscellaneous; OV: Ovarian serous cystadenocarcinoma; PAAD: Pancreatic adenocarcinoma; PCPG: Pheochromocytoma and Paraganglioma; PRAD: Prostate adenocarcinoma; READ: Rectum adenocarcinoma; SARC: Sarcoma; SKCM: Skin Cutaneous Melanoma; STAD: Stomach adenocarcinoma; TGCT: Testicular Germ Cell Tumors; THYM: Thymoma; THCA: Thyroid carcinoma; UCS: Uterine Carcinosarcoma. (B-D) Expression levels 22 of FLCN (B), FNIP1 (C) and FNIP2 (D) in the different molecular subtypes of breast cancer in the TCGA dataset, as defined by the PAM50/AIMS (prediction analysis of microarray 50) gene signature. Significance was determined using one-way ANOVA with application of the Bonferroni correction (**$p<0.01$, ***$p<0.001$, ****$p<0.0001$). (E) Immunohistochemistry analysis of human GPNMB for the selected patient derived xenografts (PDXs) representing the functional

FLCN/FNIP1/2 complex in green (1738 and 1828) and the deregulated FLCN-FNIP1/2 complex in red (1868 and 1882). Scale bar represents 50 μm. (F) Transcript levels of human *GPNMB* in the selected patient-derived xenografts (PDXs) indicated in (E). (G) FLCN expression levels in 51 different breast cancer cell lines stratified into luminal and basal subtypes, data was obtained and analyzed from Cancer Cell. 2006 Dec; 10(6): 515–527. (H) Representative immunofluorescence images showing the localization of TFE3 in luminal (T47D and MCF7) and Triple negative breast cancer (TNBC) (MDA-MB-436 and MD-MB-157) cells. Scale bar represents 20μm.

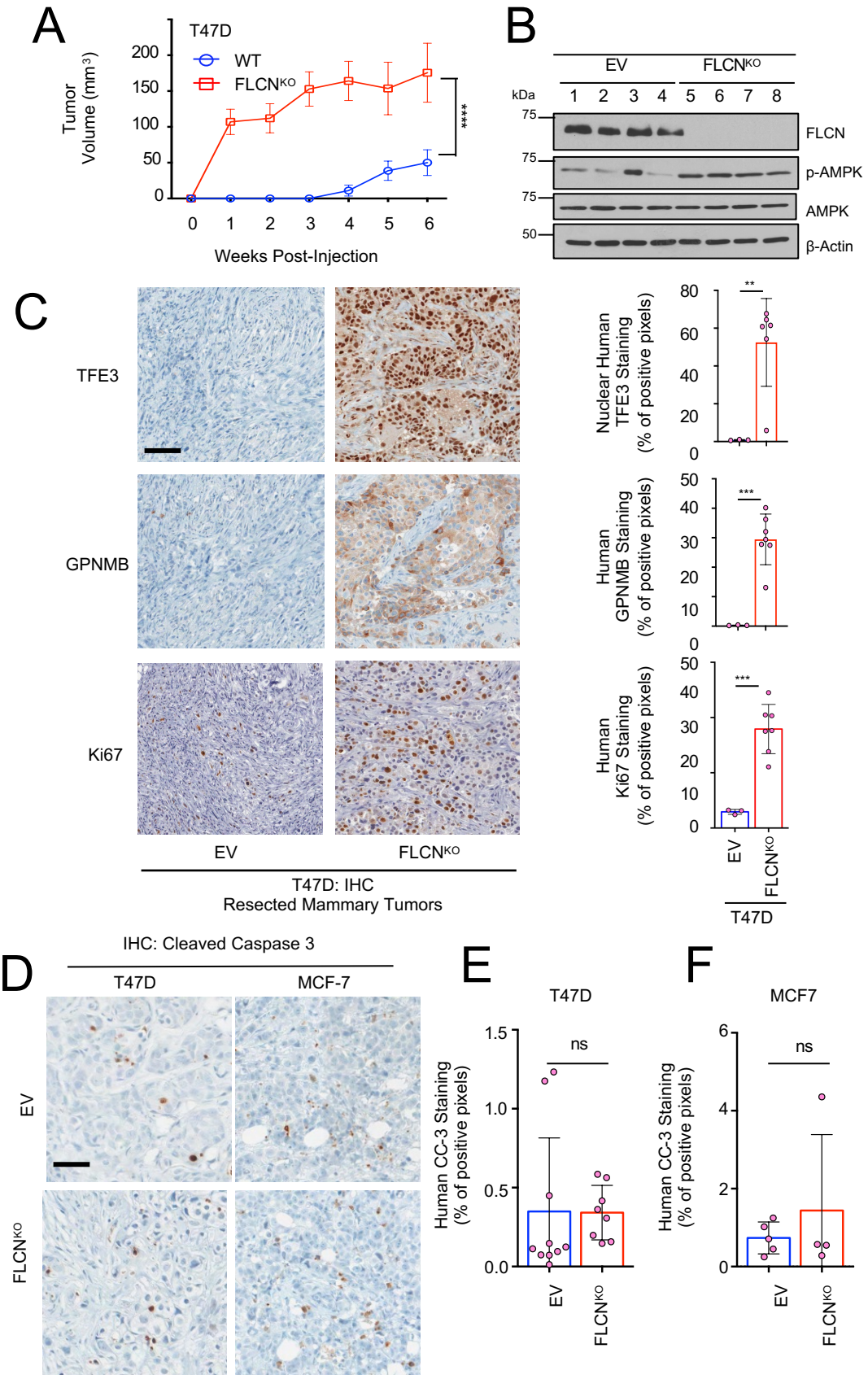
A
T47D
WT
FLCNKO
Tumor Volume (mm3)
200
150
100
50
0
0 1 2 3 4 5 6
Weeks Post-Injection
****
B
EV
FLCNKO
kDa
1 2 3 4 5 6 7 8
75
75
75
50
FLCN
p-AMPK
AMPK
β-Actin
C
TFE3
GPNMB
Ki67
EV
FLCNKO
T47D: IHC
Resected Mammary Tumors
Nuclear Human TFE3 Staining (% of positive pixels)
Human GPNMB Staining (% of positive pixels)
Human Ki67 Staining (% of positive pixels)
**
***
***
EV
FLCNKO
T47D
D
IHC: Cleaved Caspase 3
T47D
MCF-7
EV
FLCNKO
E
T47D
Human CC-3 Staining (% of positive pixels)
1.5
1.0
0.5
0.0
ns
EV
FLCNKO
F
MCF7
Human CC-3 Staining (% of positive pixels)
6
4
2
0
ns
EV
FLCNKO

33

Supplemental Figure 2 (related to Figure 4). **Loss of FLCN in luminal breast cancer cells enhances tumor growth.** (A) Growth curves of tumors of empty vector (EV) (blue) and FLCN knock out ($FLCN^{KO}$) (red) T47D cells injected in mammary fat pad (MFP) of NSG mice over the course of 7 weeks. Data represents the mean volumes of mice in each cohort measured each week (n=10 in each cohort) ± SEM. Significance was determined using repeated measures one-way ANOVA on prism (****$p<0.0001$). (B) Immunoblot analysis of EV and $FLCN^{KO}$ T47D tumor lysates resected 7 weeks post-injection. Four representative samples were run from each cohort. Actin was used as a loading control. (C) Representative images of the immunohistochemistry (IHC) staining for TFE3, GPNMB and Ki67 of EV and $FLCN^{KO}$ re-expressing FLCN T47D tumors resected 7 weeks post-injection. Scale bar represents 50 μm (left). Quantification of IHC results showing the percentage TFE3 nuclear localization, positive GPNMB staining and positive Ki67 staining, in the EV and $FLCN^{KO}$ T47D tumors (right). Data represents mean quantifications of IHC images from at least 3 different mice ± SEM. Significance was determined using Student's t-test (***$p<0.001$, **$p<0.01$). (D) Representative IHC of cleaved caspase-3 staining in EV and $FLCN^{KO}$ tumors resected from mice injected with T47D or MCF7 cells on week 6 and 5, respectively. Scale bar represents 50 μm. Quantification of IHC results showing the positive cleaved caspase-3 staining in T47D and MCF7 cells, in the EV and $FLCN^{KO}$ tumors. Data represents mean quantifications of IHC images from at least 3 different mice ± SEM. Significance was determined using Student's t-test (ns=non-significant).

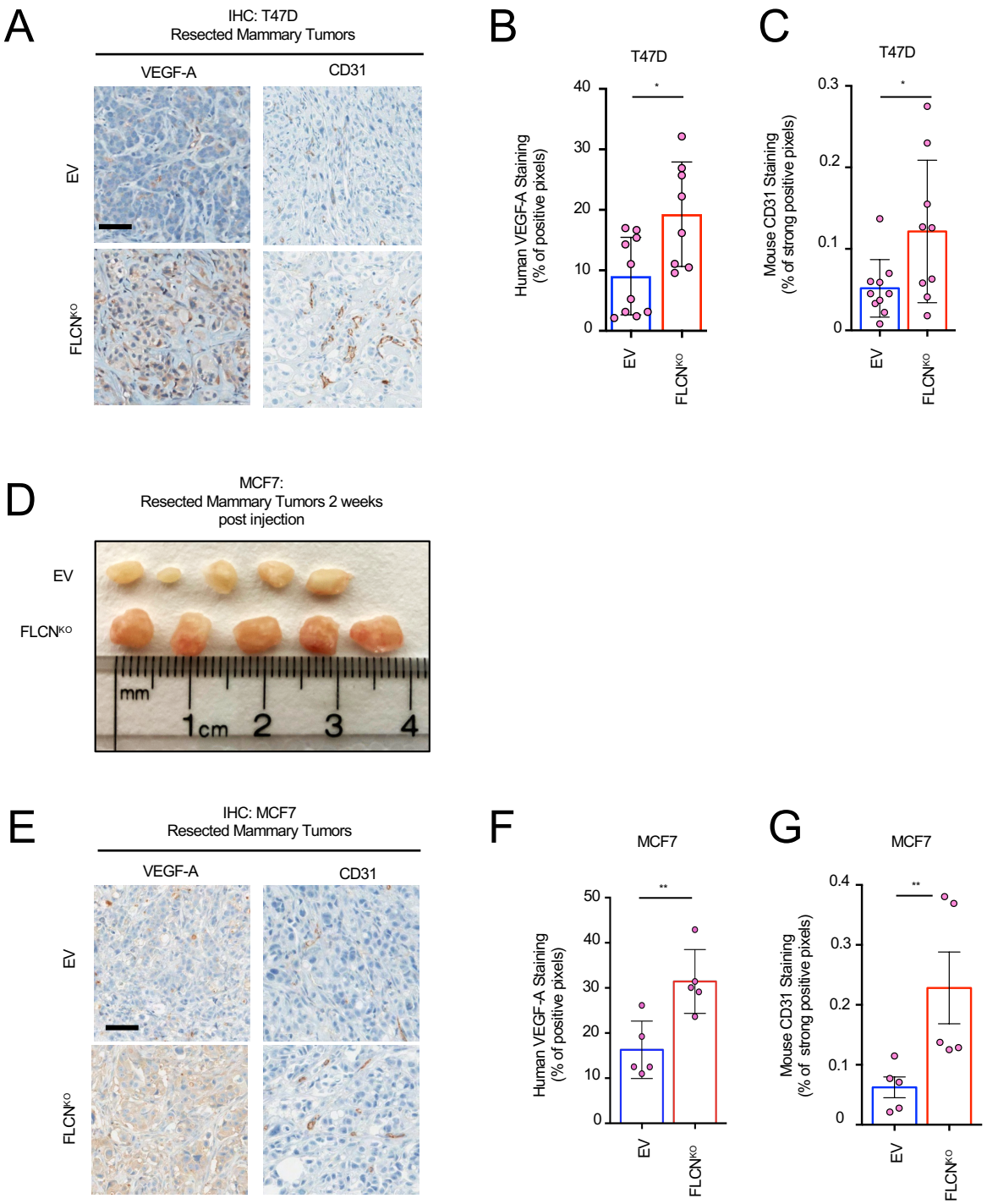

Supplemental Figure 3 (related to Figure 5). **Loss of FLCN in luminal breast cancer cells induces an angiogenic response.** (A) Representative images of the immunohistochemistry (IHC) staining for human VEGF-A and mouse CD31 of empty vector (EV) and FLCN knock out

(FLCN^{KO}) T47D tumors resected 7 weeks post-injection. Scale bar represents 50 μm. (B, C) Quantification of IHC results in (A) showing % positive VEGF-A staining (B) and positive CD31 staining (C) in EV and FLCN^{KO} T47D tumors. Data represents mean quantifications of IHC images from at least 9 different mice ± SEM. Significance was determined using Student's t-test (**p<0.01). (D) Photograph image of MCF7 EV and FLCN^{KO} mammary fat pad tumors resected 2 weeks post-injection. (E) Representative images of the immunohistochemistry (IHC) staining for human VEGF-A of EV and mouse CD31 and FLCN^{KO} tumors resected 2 weeks post-injection. Scale bar represents 50 μm. (F) Quantification of IHC results in (E) showing % positive VEGF-A staining (F) and positive CD31 staining (G) in EV and FLCN^{KO} MCF7 tumors. Data represents mean quantifications of IHC images from at least 5 different mice ± SEM. Significance was determined using Student's t-test **p<0.01). Heatmap representing differential gene expression of tumor secreted chemoattractants in WT and FLCN^{KO} MCF7 tumors following RNA-sequencing analysis. Each column represents a different mouse from each cohort, where blue is WT and red is FLCN^{KO}. Fold increase was normalized against EV and color-coded (dark red indicates 3-fold or more increase, light green indicates 3-fold or more decrease, black indicates no change).

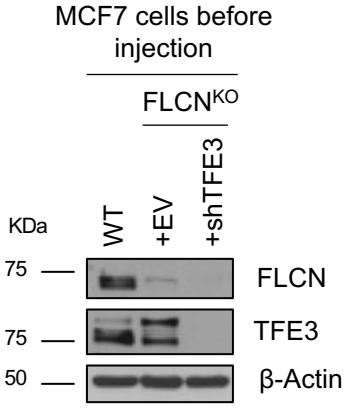

Supplemental Figure 4 (related to Figure 6). **Validation of TFE3 and FLCN levels in MCF7 breast cancer cells prior to injection**. (A) Immunoblot analysis of TFE3 and FLCN levels in wild

type (WT), FLCN KO (FLCN^{KO}) +EV, and FLCN KO +shTFE3 MCF7 cells before injection. Actin was used as a loading control.

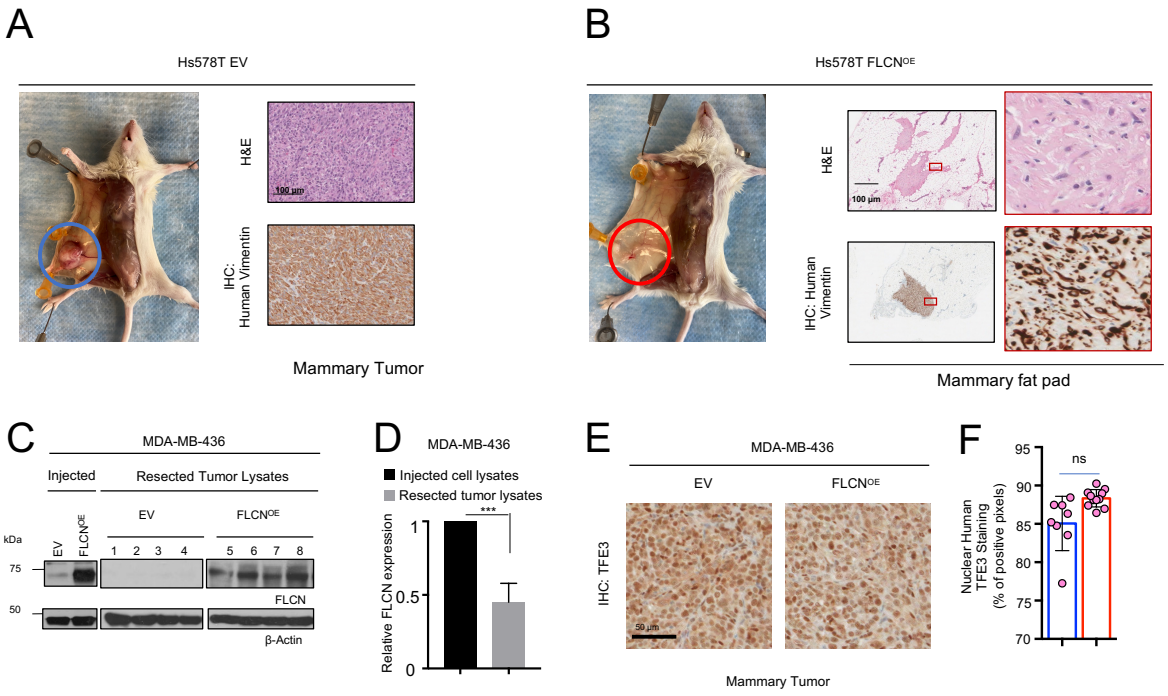

Supplemental Figure 5 (related to Figure 8)**. FLCN overexpression in basal-like breast cancer cells**. (A) Representative images of mice injected with Hs578T empty vector (EV) cells, highlighting the tumor in the mammary fat pad (blue circle, left image). Representative images of H&E and immunohistochemistry (IHC) staining for human vimentin in Hs578T EV cells tumors resected 6 weeks post-injection (right). Scale bar represents 100 µm. (B) Representative images of mice injected with Hs578T FLCN overexpressing (FLCN^{OE}) cells, highlighting the mammary fat pad containing residual cancer cells (red circle, left image). Representative images of H&E and IHC staining for human vimentin, revealing residual cancer cells, in the mammary fat pad of the mice injected with Hs578T FLCN^{OE} cells resected 6 weeks post-injection (right). Scale bar represents 100 µm. (C) Immunoblot analysis of EV and FLCN^{OE} MDA-MB-436 cells prior to injection (this blot is identical to the one used in Figure 8A) and in end-stage tumors. Four

representative samples were run from the FLCN^{OE} MDA-MB-436 tumors. β-Actin was used as a loading control. (D) Relative FLCN expression in samples indicated in (C) as quantified by ImageJ. Significance was determined using Student's t-test (***p<0.001). (E) Representative images of IHC staining for human TFE3 in EV and FLCN^{OE} MDA-MB-436 tumors in end-stage tumors (left). Scale bar represents 50 μm. (F) Quantitative analysis of the IHC results in (E), showing the % of TFE3 nuclear localization in EV and FLCN^{OE} MDA-MB-436 cells. Results represent the mean of the results from at least 7 mice ± SEM. Significance was determined using Student's t-test (ns=non-significant).

Supplemental Table 1 (related to Figures 2, 3, 5, and 7): Oligonucleotide sequences of the human primers used for qPCR

Gene	Forward primer	Reverse primer
ATP6V0E1	CTCACTGTGCCTCTCATTGTG	CACCAACATGGTAATGATAACTCC
ASAH1	AGTTGCGTCGCCTTAGTCCT	TGCACCTCTGTACGTTGGTC
TPP1	GGGAGGACCAGGAGCAT	GGGCCTAGAGAGCTCAGAAT
MCOLIN1	TAGCGACTGCCTTCGACCC	GCCCTTTTCTCCACCGTGA
TFEB	CGGACAGATTGACCTTCAGAG	GCTGCTGCTGTTGCATATAAT
TFE3	CCGTGTTCGTGCTGTTGGA	CTCGTAGAAGCTGTCAGGAT
SLCA1	GAAGCAGTGGCAGCGGTGTTTATT	ATGTGGCCGTGATACTGATGGTGA
LDHA	CTCCAAGCTGGTCATTATCACG	AGTTCGGGCTGTATTTTACAACA
HK-2	GAGCCACCACTCACCCTACT	ACCCAAAGCACACGGAAGTT
ATPV1C1	ATTGCATGCGGCAACTTCAA	CCAAGACATCCAACGTGCCA
PGC1-α	GTGTGTGCTGTGTG TCAGAGTGG	GAGTCTTGGCTGCACATGTCCC

ATP5J	TCAGCCGTCTCAGTCCATTT	CCAAACATTTGCTTGAGCTT
PGC1-β	CTCTTCACCCTGCCACTCC	ACCTCGCACTCCTCAATCTC
VEGF-α	AGGCCAGCACATAGGAGAGA	TACCGGGATTTCTTGCGCTT
ENO1	CTGGTGCCGTTGAGAAGGG	GGTTGTGGTAAACCTCTGCTC
TBP	AGGGTTTCTGGTTTGCCAAGA	CTGAATAGGCTGTGGGGTCA

Supplemental Table S2 (related to Figure 5). RNA-sequencing results of the complete list of differentially expressed genes in wild type (WT) compared to FLCN knock out ($FLCN^{KO}$) MCF7 cells.

Supplemental Table S3 (related to Figure 5). Complete GO enrichment list in FLCN knock out ($FLCN^{KO}$) MCF7 cells through enrichment of functionally annotated gene sets among the differentially expressed genes.